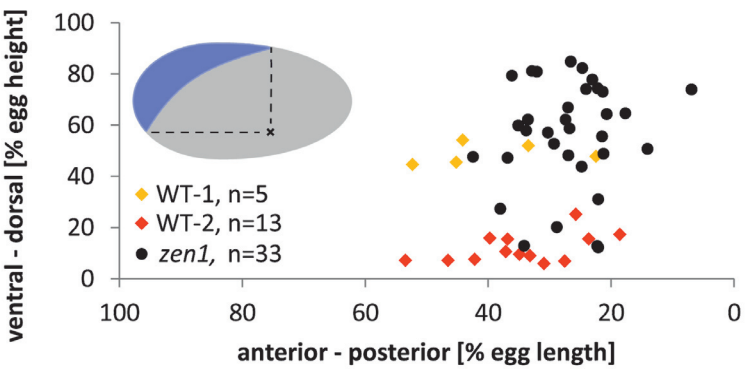

Fig. S1. Spatial analysis of early *Tc-Doc* expression in wild type and after *Tc-zen1*^{RNAi}. As *Tc-zen1*^{RNAi} embryos lack the serosa, we were not able to stage the embryos by the formation of the differentiated blastoderm. To compare early *Tc-Doc* expression between wild type and *Tc-zen1*^{RNAi} embryos we therefore recorded the maximum extension of *Tc-Doc* mRNA along the anterior-posterior and the dorsal-ventral axes. We compared wild type undifferentiated blastoderm eggs to *Tc-zen1*^{RNAi} eggs before formation of a primitive pit (therefore including stages that would be differentiated blastoderm in wild type). We found two distinct phases in wild type expression, based on the ventral extent of the expression domain (WT-1 and WT-2). WT-1 corresponds to the early stage when expression is more dorsal, while in WT-2 the expression already expands ventrally towards the edge of the presumptive serosal domain, presumably under the control of *Tc-zen1*. In contrast, *Tc-Doc* expression after *Tc-zen1*^{RNAi} remains dorsal, similar to the WT-1 category.

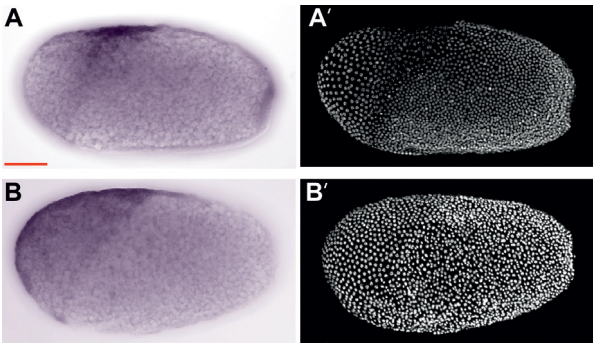

Fig. S2. *Tc-Doc* expression visualized by different *in situ* probes. *Tc-Doc* expression in the differentiated blastoderm has previously been reported to mark the dorsal part of the serosa (van der Zee et al., 2006). Here, we report expression throughout the whole serosa, albeit slightly weaker ventrally. This discrepancy can be explained by the different *in situ* probes used here and in van der Zee et al. (2006). **(A)** *Tc-Doc in situ* staining using the original plasmid to synthesize the 518-bp probe used by van der Zee, including a 60 bp intron. **(B)** *Tc-Doc in situ* using a 654-bp exon-only probe in the same experiment. Note that colorimetric detection of the probe took approximately twice the time in A as in B, arguing for a higher sensitivity of the longer probe used in this study. Primer sequence details for both probes are given in Table S1. All images are lateral views with anterior left. The red scale bar is 100 µm.

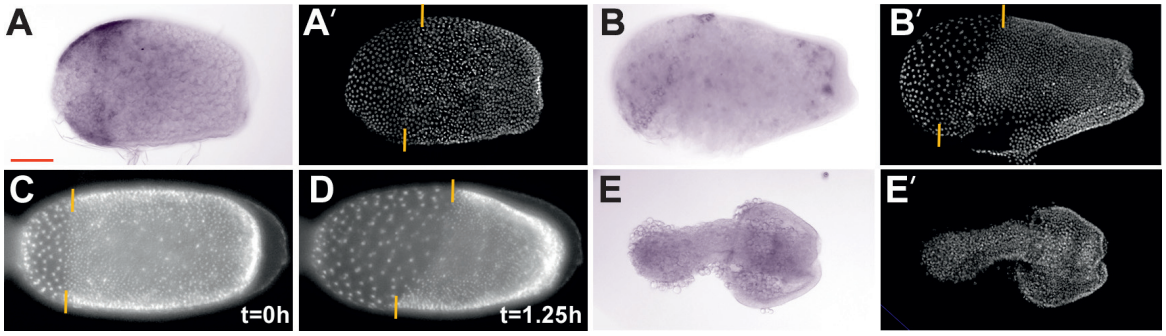

Fig. S3. *Tc-dpp*^{RNAi} embryos show a transient oblique border between the serosa and germ rudiment, with *Tc-Doc* expression only in the serosa. Knockdown of *Tc-dpp* has been reported to result in a straight border between the serosa and the germ rudiment due to complete ventralization of the blastoderm (van der Zee et al., 2006). In our experiments this was true for 85% of embryos at the differentiated blastoderm stage (n=13). However, live imaging shows that the straight border can transiently shift to an oblique conformation, reminiscent of the WT border shape, before ectopic invagination at the posterior pole occurs. This transient stage was chosen for Fig. 1F, because it shows the two key features of (1) wild type-like dynamics of *Tc-Doc* expression in retracting towards the border after the differentiated blastoderm stage and (2) the lack of *Tc-Doc* expression in the posterior amniotic fold. All images show *Tc-dpp*^{RNAi} embryos; A, B and E are *Tc-Doc in situ* staining; C and D show nuclear GFP signal from live imaging recordings. Note that serosal *Tc-Doc* expression in *Tc-dpp*^{RNAi} appears weaker than in WT (compare with main text Fig. 1). However, due to the ventralization phenotype of *Tc-dpp*^{RNAi}, serosal expression in these embryos should be compared to expression in the ventral part of WT serosa, which is weaker. In our experiments we did not find evidence for a significant difference in staining between the WT ventral serosa and the *Tc-dpp*^{RNAi} ventralized serosa. **(A)** *Tc-Doc* expression in the differentiated blastoderm stage is restricted to the serosa, which forms a straight border with the germ rudiment. **(B, reproduced from Fig. 1)** *Tc-Doc* expression retracts to the border, which is oblique during the posterior amniotic fold stage as the germ rudiment invaginates at the posterior pole. **(C, D)** Stills from live imaging of a representative *Tc-dpp*^{RNAi} embryo, showing a shift of the border from straight to oblique before posterior invagination (not shown). **(E)** During invagination, the posterior of the embryo forms a tube-like structure within the yolk while the anterior part remains at the surface of the egg (compare with van der Zee et al., 2006, supporting figures 12 and 13). Note that the serosa and yolk have been removed during fixation and there is no detectable *Tc-Doc* expression in the remaining tissues. The penetrance of this defect was 100% (n=12). All images are oriented with anterior left, and shown in lateral views where it could be determined. The orange lines demarcate the border between serosa and germ rudiment. The red scale bar is 100 μm. Embryonic material in A, B and E was a gift from Nadine Frey, from an RNAi experiment in which the expression of *Tc-dpp* itself and also of *Tc-Doc* were reduced by 60%, as determined by RT-qPCR (Stappert, D., Frey, N., von Levetzow, C. and Roth, S. (2016). Genome-wide identification of *Tribolium* dorsoventral patterning genes. *Development* 143, 2443-2454.).

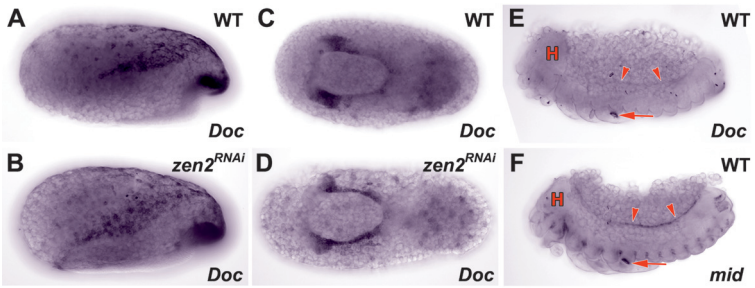

Fig. S4. *Tc-Doc* expression is not altered after *Tc-zen2*^{RNAi} and not present at the retracted germ band stage. (A, C) Wild type *Tc-Doc* expression at the posterior amniotic fold and serosal window stages (reproduced from main text Figs. 1C and 2A). **(B, D)** *Tc-Doc* expression in *Tc-zen2*^{RNAi} embryos of comparable stages is not different from wild type. **(E-F)** Although *Tc-Doc* is expressed in the early mesoderm (main text Fig. 2F), no expression could be detected at later developmental stages, including for the mesodermal derivative tissue of the cardioblast cell row (presumptive heart: red arrowheads). In contrast, the conserved cardioblast marker *Tc-mid* is expressed at this stage (F; see also Koelzer et al 2014). Note that there is unspecific staining trapped in the pleuropodia of older embryos (red arrow), a probe-independent artifact (Koelzer et al 2014). This feature was used as an internal control for the staining procedure, by allowing colorimetric staining in the pleuropodia to develop to comparable intensities for *Tc-Doc* and *Tc-mid.* All images are lateral views, except C and D, which are ventral views. Anterior is left in all images. The red scale bar is 100 µm. H, head.

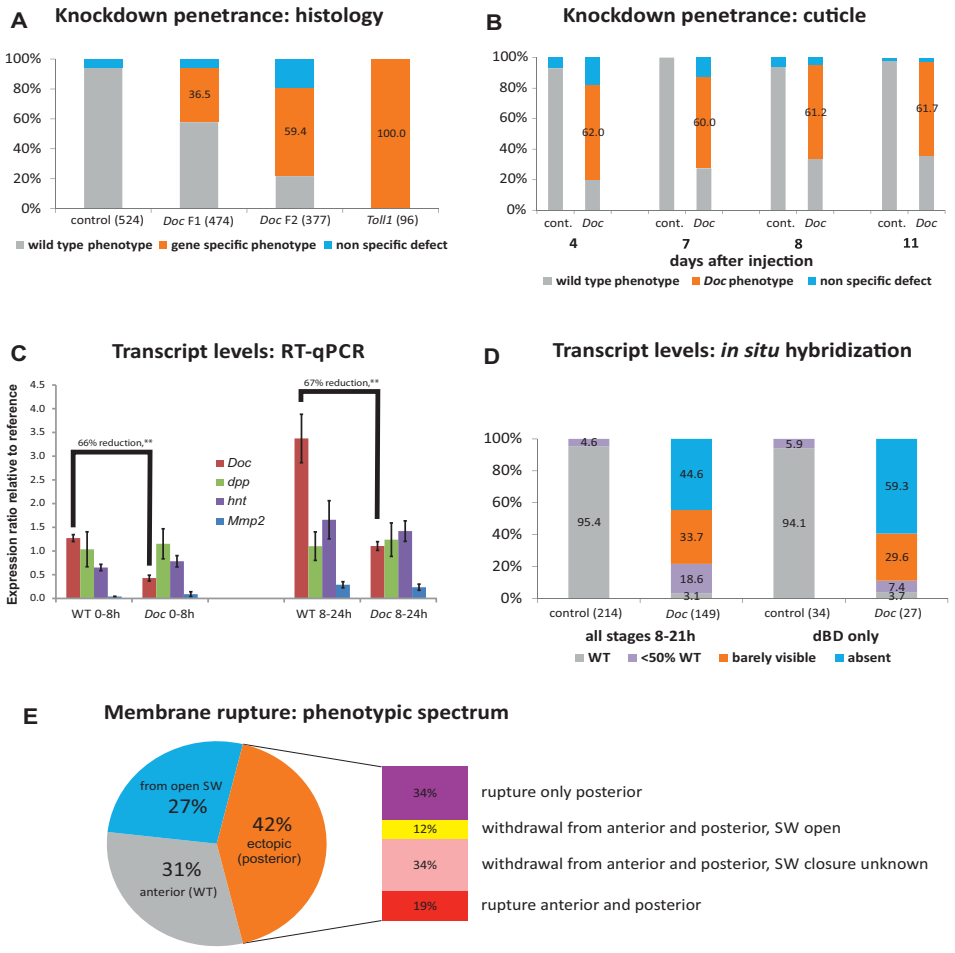

Fig. S5. Quantification of *Tc-Doc*^{RNAi} efficiency and phenotypic penetrance. (A) Comparison of two non-overlapping dsRNA fragments for *Tc-Doc*^{RNAi} (Table S1), assessed by embryonic histology with a fuchsin nuclear stain for serosal window through post-dorsal closure stages (from material collected 8-79 hAEL). Negative control embryos were from females injected with water. The positive control with *Tc-Toll1* produced 100% offspring with the *Tc-Toll1* specific phenotype (Nunes da Fonseca et al., 2008). For *Tc-Doc*, fragment F2 showed a higher penetrance than fragment F1, which was also confirmed by scoring of larval cuticle preparations from the same pRNAi experiment (*Tc-Doc* fragment F1: 33%, n= 67; *Tc-Doc* fragment F2: 67%, n= 40). Thus, fragment F2 was used for all subsequent analyses. Note that fragment F2 also generated a larger proportion of embryos with "non specific defects" than fragment F1. A fraction of this group may in fact include gene specific but milder knockdown defects, which were excluded due to the strict phenotypic scoring definitions used. Thus, the knockdown penetrance value of 59% (also shown in main text Fig. 3A) may be an underestimation. **(B)** Time course of *Tc-Doc*^{RNAi} penetrance after parental injection. The knockdown effect was stable for at least 11 days after injection, based on cuticle scoring (mean n=104, range 40-277). The data from day 8 is also shown in main text Fig. 3A. **(C)** Gene expression after *Tc-Doc*^{RNAi}, measured by RT-qPCR with the

reference gene *Tc-Ribosomal protein S3* (*Tc-RpS3*). Data are shown from three biological replicates. *Tc-Doc* mRNA levels dropped significantly (**: p<0.01 for unpaired, two-tailed *t*-test), by 66-67%, after *Tc-Doc*^{RNAi} in 0-8 and 8-24 hour old embryos, corresponding to the blastoderm stage and then to the stages from primitive pit formation through maximum germ band extension. mRNA expression of *Tc-decapentaplegic* (*Tc-dpp*), *Tc-hindsight* (*Tc-hnt*) and *Tc-Matrix metalloproteinase 2* (*Tc-Mmp2*) were not significantly changed after *Tc-Doc*^{RNAi}. **(D)** *Tc-Doc* expression examined by colorimetric *in situ* hybridization in *Tc-Doc*^{RNAi} embryos aged 8-21 hAEL. Over 94% of control embryos had strong expression that for quantification purposes was defined as "WT" levels, across all the developmental stages surveyed (left), and in particular at the key patterning stage of the differentiated blastoderm (dBD, right). A small minority showed reduced expression ("<50% of WT" strength), which may be due to experimental limitations or biological variability. In *Tc-Doc*^{RNAi}, 78% (all) and 89% (dBD only) embryos showed absent or barely visible *Tc-Doc* staining. Embryos were collected from mothers injected with dsRNA as pupae, at a concentration of approximately 0.12µg/female. **(E)** Distribution of membrane rupture defects scored by live imaging (n= 137; see main text Fig. 3B for the distribution of all defects). In 31% of the embryos, rupture occurred at the endogenous anterior position while in 27% the serosal window was not closed and membranes withdrew from there. In all cases of ectopic rupture (42%), rupture was observed from the posterior pole but varied in anterior tissue behavior (inset stacked column). Sample sizes are specified parenthetically in A and D. Abbreviations: dBD, differentiated blastoderm; SW, serosal window. Unless noted, all dsRNA was injected into adult females with approximately 0.3 µg/female.

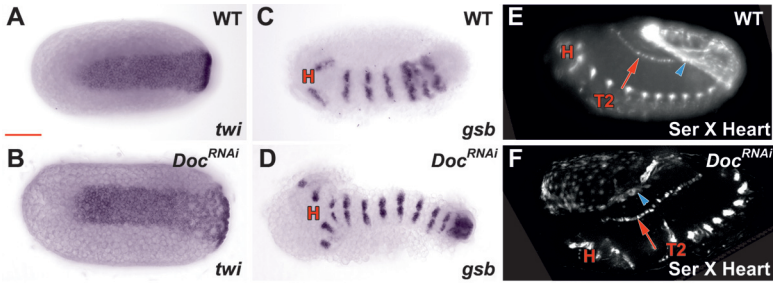

Fig. S6. Mesodermal fate, segmentation, EE tissue maintenance and cardioblast formation are unaffected by *Tc-Doc*^{RNAi}. (A-D) We used *Tc-twist* (*Tc-twi*) as a marker for mesoderm and *Tc-gooseberry* (*Tc-gsb*) as a marker of segmental development (Nunes da Fonseca et al., 2008). *in situ* hybridization in *Tc-Doc*^{RNAi} embryos did not show any defect. **(E-F)** Heterozygote cross between serosa (blue arrowhead) and cardioblast (red arrow) fluorescent marker lines (Koelzer et al., 2014). The serosal tissue persists through late EE morphogenetic rearrangements, as does the amnion (data not shown from *Tc-Doc*^{RNAi} in an amnion-GFP background, using the fluorescent transgenic line described in Hilbrant et al., 2016). Also, the cardioblast cell row was still present after *Tc-Doc*^{RNAi} (F, Movie 2). A-D are ventral views, E-F are lateral view stills from Movie 2. The red scale bar is 100 µm. H, head; Ser, serosa; T2, thoracic segment 2.

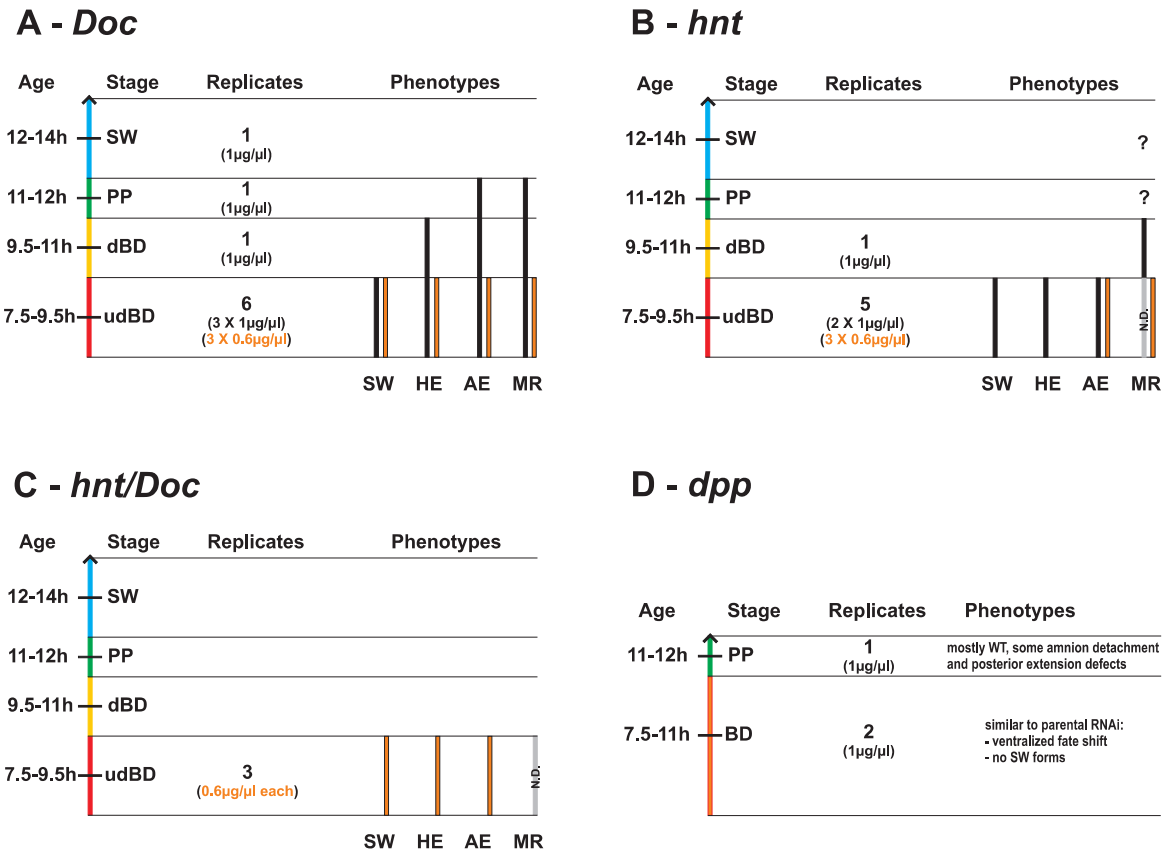

Fig. S7. Timing and obtained phenotypes from embryonic RNAi. Age and developmental stage at the time of dsRNA injection, as well as number of experimental replicates and dsRNA concentration, are indicated. Injection times are the mean of a one-hour window of egg lay. Stage abbreviations: udBD, undifferentiated blastoderm; dBD, differentiated blastoderm; PP, primitive pit stage; SW, serosal window stage. Phenotype bars indicate that at least one third of the embryos showed the corresponding phenotype after *Tc-Doc*^{RNAi} **(A)**, *Tc-hnt*^{RNAi} **(B)** and *Tc-Doc*/*Tc-hnt* double RNAi **(C)**. Phenotype bar color corresponds to dsRNA concentration. Phenotype abbreviations: SW, serosal window defect; HE, head extension defect; AE, abdominal extension defect; MR, membrane rupture defect. Developmental progression after *Tc-hnt*^{RNAi} was not monitored beyond the primitive pit stage ("?" in B), while early injected eggs in the *Tc-Doc*/ *Tc-hnt* double RNAi did not survive to rupture stage (C). **(D)** Eggs injected with *Tc-dpp* dsRNA at the blastoderm stage showed the parental RNAi phenotype (Fig. S3, see also van der Zee et al., 2006) with no serosal window forming, while eggs injected at the primitive pit stage were mostly wild type with some showing defects in anterior amnion extension and abdominal extension (see main text). Ages are shown in hours after egg lay at 30ºC. N.D., no data.

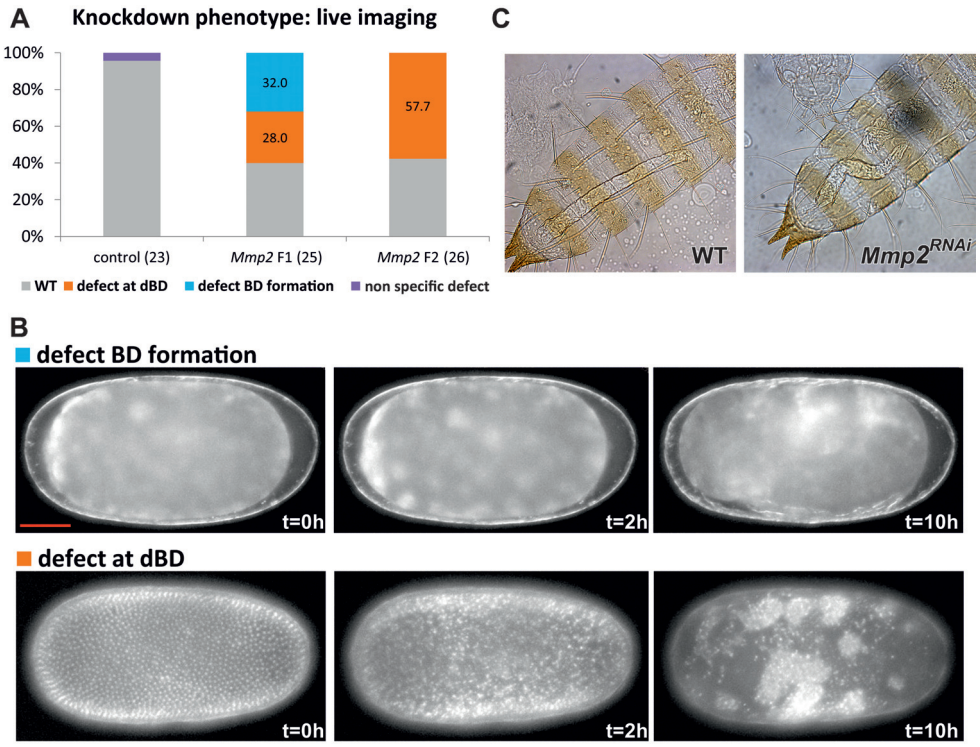

Fig. S8. Phenotype and penetrance of *Tc-Mmp2*^{RNAi}. Knockdown of *Tc-Mmp2* has previously been reported to result in only minor defects in the larval gut (Knorr et al., 2009). This is in contrast to our findings that many embryos showed severe defects at the blastoderm (BD) stage. To test for specificity, we used two non-overlapping dsRNA fragments for *Tc-Mmp2*^{RNAi} (Table S1), injecting approximately 0.2 µg dsRNA per female (the same amount Knorr et al. (2009) used). **(A)** Analysis of live imaging recordings, where 58% of the eggs failed to produce a differentiated blastoderm (dBD). However, fragment F1 seems to be slightly more severe, as nearly half of the 58% did not even form a blastoderm. **(B)** Stills from live imaging recordings showing the most severe phenotype of fragment F1, where the nuclei do not reach the surface of the egg to form a blastoderm (top), and the less severe phenotype shared by both fragments, where the undifferentiated blastoderm appears normal, but disintegrates before a differentiated blastoderm can be formed (bottom). **(C)** Consistent with the phenotype reported by Knorr et al. (2009), we observed a twisted hindgut in some of the surviving larvae. We suspect that the early lethal defects described here had escaped the authors' detection, as they inspected larval phenotypes only. It should be noted that injecting 4.8 µg dsRNA per female resulted in a penetrance of >90% for the blastoderm stage defects. BD, blastoderm; dBD, differentiated blastoderm. The red scale bar is 100 µm.

Table S1: ***Tribolium* primer sequences for RNAi, *in situ* hybridization and RT-qPCR.** All RNAi and *in situ* primers also included an adapter sequence for subsequent amplification with the T7 promoter universal primer, as described (Koelzer et al., 2014), except where marked by *. This probe was synthesized from the plasmid described by (van der Zee et al., 2006) using SP6 RNA polymerase (Roche).

RNAi			**Length**
Doc F1	forward	CCAAAAACCGTCTTTTTCCA	464 bp
	reverse	CCAGGAAGAGGCAGTAGTCG	
Doc F2	forward	TCTAAAGGCTCGCACTGGAT	469 bp
	reverse	CAGGATAAGGGCGGTAACAA	
zen1	forward	TCCCAATTTGAAAACCAAGC	688 bp
	reverse	CGTTCCACCCTTCCTGATAA	
zen2	forward	ATTACCATTCTCGGGGCTTT	374 bp
	reverse	AGTTGAGGTTTTGGGCCATT	
Mmp2 F1	forward	AAGTCCGGCTCGTCATTTC	450 bp
	reverse	GCTTGATCCTGTCCCACAAT	
Mmp2 F2	forward	CCATGCATCCCGATAAGAAG	413 bp
	reverse	GAGTCGATTTCCGGTGAAAA	
dpp	forward	AGATCGACACTGTTGCCCCTTTT	500 bp
	reverse	AGATGGTTGGTTTTGGGGTCTTG	
iro	forward	CCCGAAGTGTCGGTGTCTAC	526 bp
	reverse	TCCCGTTTGTCCTCTTCATC	
Toll1	forward	GCCGTTTCGCTCGTAACTCT	763 bp
	reverse	GTAGGGTCAAGTCGGGACATAA	
hnt	forward	TGACTTGACCAAGACGCAAG	627 bp
	reverse	GCTTTCTTGACCTCCTCACG	
***in situ* hybridization**			**Length**
Doc	forward	GAAGGCCAAATGGTCAGTGT	654 bp
	reverse	GTCGGGATGTTCGGAAACTA	
Doc (van der Zee et al., 2006)	forward	ATCCGCCGACTACTGCCTCTTCCT	518 bp (incl. 60 bp intron)*
	reverse	CTAACTGTTTCCGCTTCGCACTCG	
hnt	forward	TGACTTGACCAAGACGCAAG	627 bp
	reverse	GCTTTCTTGACCTCCTCACG	
twi	forward	GCTGATGGACCTGACCAACT	567 bp
	reverse	CTCCAATCACCCTCCATCC	
gsb	forward	GGCACCGTATTTCACTGGAT	630 bp
	reverse	GCCAGTTCTTCCCTGGTGTA	
zen2	forward	ATTACCATTCTCGGGGCTTT	818 bp
	reverse	GTGAGGTCAAGTTGGGTTGG	
dpp	forward	GTGGCATGTTGTTGGGGTAA	904 bp
	reverse	TGTGGTCTGGAATGGGGTAC	
zen1	forward	TCCCAATTTGAAAACCAAGC	688 bp
	reverse	CGTTCCACCCTTCCTGATAA	
pnr	forward	GTTCCATACAAGCGGTGGTG	1068 bp
	reverse	TCGCTTTTGATGGCACTTGT	
mid	forward	AGTTCAACGAATTGGGAACG	699 bp
	reverse	TCAGAAACAACTGCGACCTG	
Mmp2	forward	AAGTCCGGCTCGTCATTTC	1016 bp
	reverse	GAGTCGATTTCCGGTGAAAA	
iro	forward	AGTCCCACGTATCCCCTTTG	
	reverse	TCTTTCTCCTTGTCGTCGCT	
RT-qPCR			**Length** (gDNA/cDNA)
Doc	forward	GACCTGCAGACGGAGATGAT	3.784/109 bp
	reverse	CCAGGAAGAGGCAGTAGTCG	
dpp	forward	ATACGGAGCTTCACCCATGT	2.551/125 bp
	reverse	TTTATTTCGGCCGCTGTGAG	
hnt	forward	CAAGGGGTGCTCTTCATGC	3.031/133 bp
	reverse	TTTGGGTGCTTTGGTTCGTT	
Mmp2	forward	ACAATTTCCCCTTTGACGGC	2.648/153 bp
	reverse	GGGCCGCCACATTGAATAAA	
RpS3	forward	ACCTCGATACACCATAGCAAGC	186/186 bp
	reverse	ACCGTCGTATTCGTGAATTGAC	

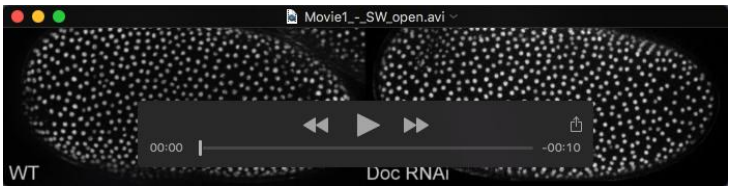

Movie 1. Serosal window closure fails after *Tc-Doc*^{RNAi}. Both embryos express nuclear-localized GFP (nGFP) ubiquitously and are shown in lateral aspect with anterior left and dorsal up. The movie shows early development of *Tribolium* including the last round of cell division in the uniform blastoderm followed by another round only in the germ rudiment (embryo and amnion). Left: wild type development showing the flattening of the posterior pole (primitive pit) followed by the formation of the posterior and later anterior amniotic folds. While the embryo invaginates, the border between the amnion and serosa forms the closing serosal window. Finally, the amnion and serosa detach from each other, releasing the embryo and the amnion into the yolk where they undergo germ band extension. For a schematic view of early development see main text Figure 8. Right: *Tc-Doc*^{RNAi} embryo showing normal cell division and invagination. However, closure of the serosal window slows down and finally stalls, tethering the head at a ventral position. Image stacks were acquired every 10 min at 24ºC and are shown as maximum intensity projections at each time point. The wild type and RNAi embryo are stage matched and shown at the same developmental rate, with elapsed time in hours and minutes indicated. See also main text Figure 4.

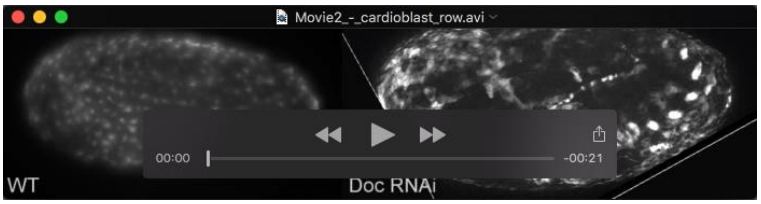

Movie 2. Serosal maintenance and cardioblast formation are unaffected by *Tc-Doc*^{RNAi}. Embryos are heterozygote crosses of enhancer trap lines that express EGFP in the serosa and embryonic domains including the cardioblast row, shown in lateral aspect with anterior left and dorsal up. The movie encompasses the late developmental stages of extraembryonic membrane rupture and withdrawal and embryonic dorsal closure. Left: wild type. Right: *Tc-Doc*^{RNAi} embryo with serosal window closure and posture defects, but with a persistent serosal tissue and wild type cardioblast row. Ultimately, dorsal closure fails in the *Tc-Doc*^{RNAi} embryo, and yolk can be seen spilling out over the embryo's head at the end of the movie. Image stacks were acquired every 10 min and are shown as maximum intensity projections at each time point. WT movie was taken at 30°C, while *Tc-Doc*^{RNAi} was taken at 24°C. See also Figure S6.

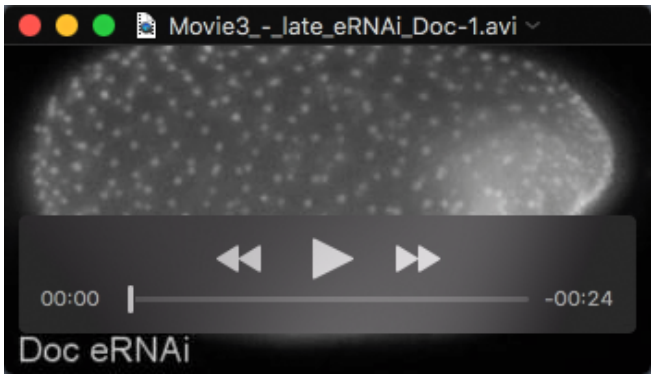

Movie 3. Later embryonic knockdown of *Tc-Doc* bypasses serosal window closure defects but still causes transient posture defects. The transgenic nuclear-GFP embryo was injected with dsRNA approximately 12h AEL and is shown in lateral aspect with anterior left and dorsal up, from serosal window closure through germ band retraction stages. Serosal window closure and anterior head extension are wild type, while posterior germ band extension is disturbed, characterized by a transient curling of the abdomen, but posture defects here are rescued during germ band retraction. Image stacks were acquired every 10 min at 30ºC and are shown as maximum intensity projections at each time point. See also main text Figure 4.

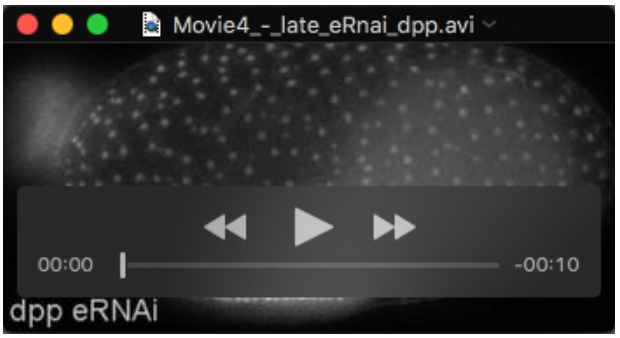

Movie 4. The *Tc-dpp*^{RNAi} phenotype after embryonic knockdown at approximately 12h AEL bypasses dorsal-ventral patterning defects but impairs morphogenesis. The transgenic nuclear-GFP embryo is shown in lateral aspect with anterior left and dorsal up, from serosal window closure through early germ band retraction stages. Serosal window closure is wild type, but the anterior amnion underneath the head shows defects, most likely due to an incomplete dissociation from the serosa. In addition, the posterior germ band extension is disturbed, characterized by a transient curling of the abdomen, similar to *Tc-Doc* embryonic RNAi. Image stacks were acquired every 10 min at 30ºC and are shown as maximum intensity projections at each time point.

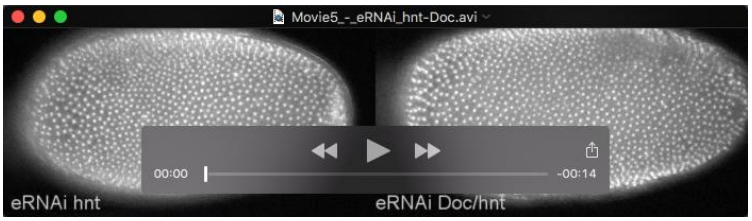

Movie 5. Loss of *Tc-hnt* or both *Tc-hnt* and *Tc-Doc* impairs serosal window closure. Embryonic RNAi against *Tc-hnt* (left) or both *Tc-hnt* and *Tc-Doc* simultaneously (right). The transgenic nuclear-GFP embryos are shown in lateral aspect with anterior left and dorsal up, from the uniform blastoderm through the extended germ band stages. Both embryos show a serosal window open phenotype similar to *Tc-Doc* RNAi alone (*cf.*, Movie 1). Note that the shape of the open serosal window was generally variable but did not differ between the three treatments. Image stacks were acquired every 10 min at 30ºC and are shown as maximum intensity projections at each time point. See also main text Figure 6.

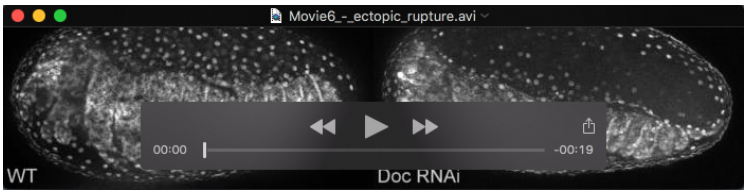

Movie 6. Extraembryonic membrane rupture defect after *Tc-Doc*^{RNAi}. The transgenic nuclear-GFP embryos are shown in lateral aspect with anterior left and dorsal up. Left: wild type rupture starts underneath the head, from where the EE membranes (only the serosa is clearly visible in the movies) pull back to the dorsal side to form the dorsal organ. Finally the back of the embryo closes during dorsal closure. Right: *Tc-Doc*^{RNAi} embryo showing ectopic rupture at the posterior pole resulting in a transient belt of extraembryonic tissue around the anterior abdomen. The formation of a functional dorsal organ fails, resulting in an incomplete extraembryonic cover over the yolk and finally lethal outflow of the yolk. Image stacks were acquired every 10 min at 30ºC and are shown as maximum intensity projections at each time point. See also main text Figure 7.

Movie 7. Dorsal closure defect after *Tc-Doc*^{RNAi}. The transgenic nuclear-GFP embryo is shown in dorsal aspect with anterior left. Extraembryonic membrane rupture and dorsal organ formation are morphologically wild type, but dorsal closure does not proceed in the posterior third of the embryo and finally the flanks of the embryo rip open again. Image stacks were acquired every 10 min at 24ºC and are shown as maximum intensity projections at each time point. See also main text Figure 7.